energies

MDPI

Article

Online Lifetime Prediction for Lithium-Ion Batteries with Cycle-by-Cycle Updates, Variance Reduction, and Model Ensembling

Calum Strange [1], Rasheed Ibraheem [1] and Gonçalo dos Reis [1,2,*]

[1] School of Mathematics, University of Edinburgh, James Clerk Maxwell Building, Peter Guthrie Tait Road, Edinburgh EH9 3FD, UK
[2] Centro de Matemática e Aplicações (CMA), Faculdade de Ciências e Tecnologia, Campus da Caparica, Universidade Nova de Lisboa, 2829-516 Caparica, Portugal
* Correspondence: G.dosReis@ed.ac.uk

Abstract: Lithium-ion batteries have found applications in many parts of our daily lives. Predicting their remaining useful life (RUL) is thus essential for management and prognostics. Most approaches look at early life prediction of RUL in the context of designing charging profiles or optimising cell design. While critical, said approaches are not directly applicable to the regular testing of cells used in applications. This article focuses on a class of models called 'one-cycle' models which are suitable for this task and characterized by versatility (in terms of online prediction frameworks and model combinations), prediction from limited input, and cells' history independence. Our contribution is fourfold. First, we show the wider deployability of the so-called one-cycle model for a different type of battery data, thus confirming its wider scope of use. Second, reflecting on how prediction models can be leveraged within battery management cloud solutions, we propose a universal Exponential-smoothing (*e*-forgetting) mechanism that leverages cycle-to-cycle prediction updates to reduce prediction variance. Third, we use this new model as a second-life assessment tool by proposing a knee region classifier. Last, using model ensembling, we build a "model of models". We show that it outperforms each underpinning model (from in-cycle variability, cycle-to-cycle variability, and empirical models). This 'ensembling' strategy allows coupling explainable and black-box methods, thus giving the user extra control over the final model.

Keywords: remaining-useful-life; prediction of full degradation curve; machine learning; cloud computing; ensemble models

Citation: Strange, C.; Ibraheem, R.; dos Reis, G. Online Lifetime Prediction for Lithium-Ion Batteries with Cycle-by-Cycle Updates, Variance Reduction, and Model Ensembling. *Energies* **2023**, *16*, 3273. https://doi.org/10.3390/en16073273

Academic Editors: Md Sazzad Hosen and Theodoros Kalogiannis

Received: 15 March 2023
Revised: 30 March 2023
Accepted: 3 April 2023
Published: 6 April 2023

1. Introduction

Data-driven models for early life prognostics regarding lithium-ion batteries (LIBs) have been studied extensively [1]. This is because LIBs are deployed into various applications, including energy storage systems and electric vehicles (EVs), and thus efficient, reliable, and accurate methods for monitoring their degradation are needed. One of the large problems here—and not the focus of this work—is the 'state of health' estimation, and approaches for it have been reviewed in [2–4]. The counterpart problem—and the focus of this paper—is the long-time prediction of life. A critical review of state-of-the-art machine learning methods for degradation prediction can be found in [2]. Further critical reviews on remaining useful life modelling include [5]—that work provides a methodology breakdown according to machine learning, filtering methods, and stochastic processes methodology. The latter methodology combines statistical theory with mathematical principles like Bayesian inference, Gaussian process regression, and others. Overall, the capability of machine learning techniques to capture hidden features for complex non-linear systems (which can be used to predict lithium-ion battery's cycle life accurately) is

unquestionable [6]. Methodologies that combine data-centric methods and physics modeling, so-called "Grey-box" models, are reviewed in [7]. This hybrid modelling approach (thus 'Grey') addresses a difficulty within the data-driven model universe: how to derive physical explanations from the dataset and results when no kinetic, chemical, or physical effects are considered. Thus, incorporating both approaches has immense value [7–9].

Models obtained via machine learning algorithms are built on battery usage data to learn the underlying degradation pattern and produce good results, especially in predicting remaining useful life (RUL) and full capacity/internal resistance (IR) curves. On the prediction of RUL, models for the identification [10] and prediction of capacity knees [10,11] and IR elbows [12] have been proposed; see [13] for an in-depth theoretical discussion of the Knee phenomena in capacity fade curves (and Elbows [12] for internal resistance). In addition, the end of life (EOL) of LIBs has been predicted with high accuracy in [9,14–16] using the health indicators extracted from the early life battery usage data. As for full trajectory prediction, from early life to end of life, for capacity degradation was considered in [17–19] where neural networks were used as the main building block. In addition, both capacity fade and IR rise curves have been jointly predicted using convolutional neural network (CNN) [20], deep recurrent neural network architecture [21], and extreme gradient boosting [22]. For instance, using CNNs for cycle-to-cycle prediction and requiring at least 100 cycles of data [17] builds a model able to predict the entire battery capacity fade curve, including the per-cycle fade rate and rollover cycle (knee point) of the capacity fade curve. Starting from the initial works [10,13], there have been outstanding contributions to knee-point identification, prediction, and classification. A deep CNN learning method was developed for online knee-point prediction under the more realistic scenario of variable battery usage [11,23]; also Ref. [24] but on a novel dataset. An original alternative, using the multitask (deep) learning method, was proposed by [21]: it uses only the information from capacity and internal resistance across 200 cycles (at least) and predicts the remaining trajectory degradation (including RUL and knees)—*no current/voltage information is used*, and this represents a significant reduction of input data.

The works mentioned above develop one single predictive model drawing on a single direct machine learning regression model. For example, in [6], machine learning and non-machine learning models are compared but not combined nor explained; a further comparison of predictive algorithms is carried in [25] via a fully automated algorithm, called H_2O AutoML, to compare and rank models according to specified metrics. Noteworthy contributions within integrated data-driven methods include [26,27], where multiple machine learning methods are sequentially *integrated* (for various subtasks) to build the final predictive model.

In effect, model comparison is a (largely) straightforward task, but *model combination* seems to remain largely unexplored in the space, i.e., what to do when multiple standalone predictive models are available for the same task? Which to choose? How to choose? Should one choose? One of the contributions of this work sheds light on this issue (Section 4.4 below).

Explainability and *interpretability* (why the high prediction accuracy) of machine learning models is a very wide issue. Zhang et al. [28] address model interpretability for lifecycle prediction via quantile regression forests (QRF). This approach allows them to build asymmetric prediction intervals without assuming any specific distribution—this is a complementary approach to the conformal prediction methodology used in [10]. Explainability analysis has been conducted in [18]; they rely on an autoregressive model to predict EOL. Their explainability analysis reports their deep model being able to learn the interplay between multiple cell degradation mechanisms. Lastly, outside the battery field and focused on deep neural networks themselves, is [29]. They address model interpretability for Deep Neural network models through a group-theoretical procedure that recasts the inner-layer signalling of the NN into a human-readable form. Deploying the procedure on a particular example, their method revealed the NN to have a surprising internal sophis-

tication, with the NN internally a range of filters and transformations. Deploying [29] to problems in the battery space is yet to be addressed.

The data needed to predict various RUL parameters and capacity/IR curves can be broadly divided into longitudinal and cross-sectional data. As for longitudinal, one means the minimum number of cycles of battery data needed to achieve a competitive accuracy, while cross-sectional data refers to the various measured quantities of battery chemistry. On longitudinal data, various machine learning algorithms taking the first 100 cycles of certain measured quantities (such as temperature, capacity, current, and voltage) have been developed to predict the end of life (EOL) [14,15,30–32] and full capacity curve [30,33]. Then in [10,22], only the first 50 cycles were used for the prediction of various RUL and capacity/IR predictions, with [22] using only discharge voltage under constant-current condition (a reduced cross-sectional data). This reduction is pushed further in [14,20] to train a class of models referred to as *one-cycle* models (sometimes also called 'historyless').

In the context of RUL prediction, one-cycle models predict RUL (and/or EOL) from the data contained in *one single cycle (any cycle)* and offer competitive performance from extremely limited input. One key benefit of one-cycle models is their flexibility in terms of the input cycle (as no history needs to be recorded or accessed). Because of this, as new in-cycle data becomes available, new predictions can be made and compared with old predictions. Historically the first one-cycle model seems to be [20] (using CNNs as the core regressor model), there have been further contributions exploring the concept further. For instance, many feature-based models are presented in [14]; one, in particular, is a one-cycle one (from non-longitudinal features), but such a model is not discussed. Two recent distinguishable contributions within the one-cycle context, and each with its distinct flavour, are: [34] using impedance-based forecasting and taking as input the future cycling protocol and a single electrochemical impedance spectroscopy measurement; and the other using a sequence-to-sequence (seq2seq) model to predict voltage-capacity curves (so many cycles) ahead of time [35].

The literature gaps highlighted originally in [20] *are yet to be closed*, and thus data-centric *one-cycle* predictive algorithms are still competitive. Strange et al. [20] argued that no electrochemical and physics-based model is yet able to predict the lifespan of a cell from a single cycle of input data. Starting from the Doyle–Fuller–Newman (DFN) model for lithium-ion batteries and its derivatives [36]: a DFN model parameterising from cycling data is extremely difficult (less even using only data from one single cycle) without unrealistic material assumptions: one would need stoichiometries of both electrodes that cannot be obtained from cycle data [37]; the cell would need to be dissembled as to carry specific measurements [38,39] (that may last up to 3-months). Without disassembling, one needs to rely on current–voltage response, for which case many of the parameters are not well identifiable—see [40] for a discussion on sensitivity analysis and optimal excitation for parameter identification. A method to obtain some of the relevant parameters through short-time measurement and pulse rapid nondestructive testing is given in [41].

Of importance to this study is [20] where the prediction of entire capacity/IR curves was made with one cycle of data consisting of in-cycle measurement of voltage, current, capacity, and IR values. The fact that a single cycle of data is sufficient to uncover the full degradation trajectory makes it ideal for practical applications such as edge-cloud frameworks. Such frameworks offer some form of real-time signal monitoring of systems [42] by leveraging the power of 5G and the Internet-of-things (IoT) for, say, EV fleet management [43–45] or stationary energy-storage assets [46,47]. The power of 5G and Internet-of-things (IoT) will unlock new innovative services for enterprises to accelerate their transformation toward Industry 4.0 as they evolve and adopt diverse new business models [48,49]. Prime advantages of IoT and cloud computing technologies include powerful computing and unlimited cloud support that results in rapid development, extended scalability, and greater visibility. As ever, there are drawbacks. The employment of a cyber-physical system leads to cyber-attack, as the system is always connected to the network. There are also implementation and maintenance costs [50]. In the past years,

the battery energy industry has become a prospective IoT application. Recent research work on improving battery capacity and RUL predictions based on a cloud framework has shown promising results [19,51–54]. In order to alleviate the computation load and power consumption in the cloud and improve communication throughput and latency, the computations are distributed to the edge to leverage locality [55–57]—with [58] proposing to attain cost efficiency in serverless machine learning training. As playing a key role in IoT applications, the power grid and distribution industry has employed edge-cloud technology to promote smart grid and improve real-time monitoring, prediction, and optimisation of power systems and distributions [55–57,59], and to address related security issues [60]. In recent surveys, vehicular edge-computing and multi-access edge computing (MEC) to guarantee energy-efficient computation and consumption to offload heavy tasks from vehicle battery to the edge to prolong battery life [61,62], which leads to new challenges to the battery energy industry and opportunities to optimise battery life prediction in the larger platform of edge-computing. Thus, in this study, we propose a framework where the model developed in [20] can be implemented in an edge-cloud paradigm facilitating quick online prediction.

Last, and to support further the vision of IoT monitoring systems underpinned by bulk cell modelling and showcasing prognostics and diagnostics tools, we point to the recent work [47] (associated to [46]). There, the authors build a battery model (in the vein of a "digital twin") with around ≈20 K individual cell models running for multiple (virtual) years and investigated degradation in their grid battery. Their key findings are that *thermal management design and control* are critical, emphasising that systems engineering matters! An independent discussion on recent advances in thermal management can be found in [63].

The rest of this study is organised as follows. Section 2 provides insight into the data used for this study, and Section 3 provides the modelling process. We provide model results with their corresponding discussions in Section 4, and concluding remarks are presented in Section 5.

2. Data Description

In this work, we consider two datasets. The first is the (RWTH Aachen University) dataset created in Baumhöfer [64] and made available at [65]—throughout this work, we make reference to this dataset as the 'Baumhöfer dataset'. The dataset belongs to the high-throughput battery cycling data class [66] (Section 2.1). Versions of this dataset have been used by the RWTH-Aachen group in multiple works and a subset appeared in [19] (in-depth data description provided in [19] (Section 2), see also [67] (Figure 3)). The dataset contains cycling data of 48 nominally identical Panasonic/Sanyo NMC/Carbon UR18650E Li-ion cells with nominal capacity 1.85 Ah. The cells were cycled at a fixed room temperature ($T = 25$ °C). The dataset contains in-cycle measurements of current, voltage, and temperature, for cells cycled at constant current on charge and discharge and last for 900–1400 cycles. Reference performance testing was carried out every so often to measure capacity and internal resistance. The data here spans past what would usually be considered the EOL for the cells. For the purpose of this study, we only consider data up to 70% of initial capacity, and in relation to this dataset, we consider 70% SOH as the EOL.

The second dataset that we consider is the block-pair Severson [15] and Attia [68] datasets (on which [20] was developed) containing 169 cells of type: A123 APR18650 M1 A, LFP/graphite, with 1.1 Ah nominal capacity. For these datasets, the cells were tested under varying fast-charging policies, which resulted in a large variability in degradation. We refer throughout to the combination of both sets the '*Severson–Attia dataset*'. The Severson–Attia datasets contain in-cycle measurements of current, voltage, and temperature and per-cycle measurements of Capacity and IR lasting from 400 to 1400 cycles. The Attia dataset does not contain measurements of IR, but synthesised data is available from a model trained on the Severson dataset and then transferred onto [12]. For this dataset and in line with previous works [16,69], we restrict our consideration to cells lasting no more than 1200 cycles; this

is due to the very small number of cells with lifetimes lasting longer than this (no more than 10).

These two datasets differ in the driving factor of cell-to-cell variability [67,69]. For the Baumhöfer dataset, as all cells are cycled in the same manner, the main driver of variability is the intrinsic manufacturing variability. In contrast, the Severson–Attia datasets consider a large variety of fast charging protocols; thus, a significant driver of variability in these datasets is extrinsic. In the view of the authors, a model accurately predicting on both types of datasets is evidence that the model captures intrinsic signs of cell degradation and is not simply learning a map between charge/discharge profiles and cycle-life.

It should be noted that the IR measurements provided with the Baumhöfer dataset are very limited (as low as 3–4 measurements over the lifetime for some cells); we thus work with a 'piecewise cubic Hermite interpolation' of the data. For this reason, the results presented here in relation to the IR are only meant to serve an indicative purpose and the majority of this work focuses on the capacity data.

3. Model Description and Associated Methodology

In the literature, there exist multiple approaches to predict the RUL, ranging from models drawing from in-cycle variability [14,20], from cycle-to-cycle variability [10,15,16], summary information such as capacity and IR measurements [19,21] and empirical models [70] among others. Each of these approaches has shown strong predictive efficacy. Thus, when the data is available (as one would have within an edge-cloud framework), it makes sense to consider a wide range of signals—we consider three models, one from each of the above approaches.

3.1. Model from In-Cycle Variability

The main model used in this work is the one-cycle CNN-based predictor model proposed in [20]; there, the model was trained for the Severson–Attia dataset, and here, we train an additional version with the Baumhöfer dataset, and (thus we use two embodiments of the one-cycle model).

Overall, the model uses the voltage and current curves from a single cycle (any cycle) as input to predict full capacity/IR trajectory (including RUL) via certain cogent points on the capacity/IR curve. Concretely, this model was trained to predict the *time to knee-onset* (ttk-o), *time to knee-point* (ttk-p), *remaining useful life* (RUL), *capacity at knee-onset* (Q@k-o), and *capacity at knee-point* (Q@k-p)—the methodology is described in [20,22]. In addition, for the Baumhöfer dataset, we predict the *time to elbow-onset* (tte-o), *time to elbow-point* (tte-p), and their corresponding IR values (IR@e-o and IR@e-p); see Table 1 for a summary.

For the Severson–Attia dataset, the model presented in [20] is deployed here *as is presented there*. For the Baumhöfer dataset, the model's hyperparameters were further tuned: increasing the number of convolutional filters in the hidden layers (comparing with the conv1d layers in [20] (Table 1)the filter numbers were set at 32, 32, 32, 64, 64, 64, 64, 64), increasing the number of training epochs to 200, increasing the dropout used to 0.45 and increasing the 'decay step' to 10 epochs.

We refer the reader to [20] (Section 3), where the underpinning CNN model is fully described and discussed (including parameter choices and their impact)—we omit such a discussion here. For the Baumhöfer dataset model training, the model is directly redeployed from [20], and the parameters (number of filters, training epochs, dropout rate) were increased in an unoptimised way—we recall that the goal of this work not an in-depth exploration of the one-cycle model from machine learning parameter optimality.

Table 1. Summary of the targets predicted by the one-cycle CNN-based model [20] (also [22]).

Predictions	Category
ttk-o, ttk-p, tte-o, tte-p, RUL	Time-to (Cycles)
Q@k-o, Q@k-p, IR@e-o, IR@e-p	Capacity (Ah)/IR values (Ω)

3.2. Model from In-Cycle Variability with Exponential-Smoothing-Memory (e-Forgetting)

In the edge-cloud/online framework, past cell information can be stored and incorporated into current predictions and diagnostics. For the one-cycle model, a natural and storage-space efficient approach is to store past predictions and then build an averaged *smoothed* prediction that reduces the variance of the final estimator.

To this end, we overlay an exponential smoothing memory step into the one-cycle predictions (when multiple predictions can be made) and coin the new model the '*e-forgetting one-cycle model*'.

Concretely, assume the one-cycle model has been trained (Section 3.1) and is now available for predictions. Assume that a new cell is being cycled/used and from time to time data of its high-throughput cycling is recorded and predictions are made. Let $(y_i)_{i=1}^{n}$ (with $n \geq 1$) be a series containing predictions of the time-to-an-event (e.g., ttk-o, ttk-p, or RUL) made at n sequential cycles (possibly the last n-cycles). For example, assume that at every 50-cycles data is recorded and an EoL prediction is made; thus, by cycle 250, one has $n = 5$ predictions $y_1, y_2, \ldots, y_5$ of EOL available.

Then, for a smoothing parameter $\lambda \in [0, 1)$, with n predictions available, one defines the *exponentially smoothed prediction* as

$$y^e(n;\lambda) := \frac{\sum_{i=0}^{n-1}(1-\lambda)^i(y_{n-i}-i)}{\sum_{i=0}^{n-1}(1-\lambda)^i} \qquad \text{where} \qquad \sum_{i=0}^{n-1}(1-\lambda)^i = \frac{1-(1-\lambda)^n}{\lambda}. \quad (1)$$

Following the example above, at cycle 250, one now has an EOL prediction given by y_5 but also one given by $y^e(5;\lambda)$.

In this way, past information can be incorporated into current predictions without storing the complete history of the cell. All that is required are the predictions from past cycles, not the data from which they were made.

The main benefit of the *e*-smoothing procedure, $y^e(n;\lambda)$, is an active reduction of the noise's influence on the prediction. Intuitively, by averaging, the outlier predictions will be smoothed out, and the variance of the estimator $y^e(5;\lambda)$ is smaller than y_5. The exponential smoothing or *e*-forgetting recognises that the prediction y_5 should be more accurate than the prediction y_4 simply because at $n = 5$ one is closer to the EOL than at $n = 4$ (see [20] (Figure 5)), thus we weight more the most recent predictions.

We note that the parameter n is a system-input choice interpreted as how far into the past one is accounting for the earlier predictions. The exponential smoothing parameter λ can be (ad-hoc) directly selected or optimised/learned via a k-fold validation approach on the training data (with the best rate λ chosen as the one which minimizes the error over the validation folds (averaged)). Lastly, a quick computation shows that with $\lambda = 0.6$ and $n = 10$, the weight of the 10th element in the sum of Equation (1) is of order 10^{-5}; this indicates that one does not need to store many past predictions.

3.3. Model from Cycle-to-Cycle Variability

For a model based on cycle-to-cycle variability, we consider the Relevance Vector Machine (RVM) based model proposed by [10]—this is a feature-based regression model. This model takes as input features generated from the differences in in-cycle data between an early-life cycle and a cycle measured later. For this work, we consider only cycles 10 and 200 to serve an illustrative purpose (the original work [10] considered cycles 10 and 50). For the online framework, it is feasible to create multiple models of this form based on gradients from different cycles. For example, models from cycle 10–50, 50–100, 100–150, and so on.

3.4. Model from Summary Information (Lookup Model)

We propose a simplistic lookup-based model to predict EOL. The lookup model compares the available (up to, say, cycle 200) capacity measurements for a cell against that of example cells with known cycle life—the comparison is made according to a preferred

metric e.g., (3), (4) or (5)—here, (3) is used. The EOL prediction for the new cell is that of the closest cell or an average of the k-th closest cells. The latter option is employed with $k = 3$.

4. Model Performance

4.1. Performance Metrics (not Online Framework)

Performance metrics for the one-cycle model predicting on the Severson–Attia dataset can be found in [20] (Tables 2 and 3). For comparison, and to confirm the robustness of the one-cycle model, we present here performance metrics for the Baumhöfer dataset. Table 2 displays the error metrics for the time-to predictions. Table 3 displays the errors for predicting capacity and IR at values. The model shows comparable performance as was found for the Severson–Attia dataset. In addition, the model generally predicts time-to targets associated with the capacity curve more accurate than those of IR curves (see the MAPE of Tables 2 and 3). This can be linked to the limited Baumhöfer IR data as pointed out in Section 2.

Table 2. Performance of proposed model on Baumhöfer dataset to predict Capacity's: ttk-o, ttk-p and RUL; and IR's: tte-o and tte-p. Average performance from within the first 100 cycles per test cell (10 cells).

	RMSE (Cycles)		**MAPE (%)**	
	Train	**Test**	**Train**	**Test**
ttk-o	120 ± 4.2	72 ± 7.2	10.0 ± 0.44	6.3 ± 0.56
ttk-p	130 ± 4.8	88 ± 7.3	9.0 ± 0.41	6.7 ± 0.40
RUL	110 ± 3.3	89 ± 8.4	7.3 ± 0.30	6.9 ± 0.50
tte-o	150 ± 3.75	160 ± 13.3	11.0 ± 0.44	12.0 ± 0.80
tte-p	130 ± 5.2	140 ± 9.9	7.6 ± 0.27	9.0 ± 0.53

Table 3. Performance of model to predict future capacity and IR, when current capacity/IR is known.

	RMSE		**MAPE (%)**	
	Train	**Test**	**Train**	**Test**
Q@k-o	0.027 ± 0.001	0.020 ± 0.001	1.3 ± 0.08	0.97 ± 0.07
Q@k-p	0.024 ± 0.002	0.025 ± 0.002	1.3 ± 0.10	1.2 ± 0.10
IR@e-o	$0.0030 \pm 8.5 \times 10^{-5}$	$0.0024 \pm 1.1 \times 10^{-4}$	3.3 ± 0.08	4.2 ± 0.15
IR@e-p	$0.0029 \pm 1.0 \times 10^{-4}$	$0.0032 \pm 2.2 \times 10^{-4}$	3.4 ± 0.11	4.9 ± 0.24

4.2. The One-Cycle Model in the Online Framework (with Full Curve Prediction)

In Figure 1, we display the full curve prediction results of the e-forgetting one-cycle model for both datasets on a random selection of test cells. The parameter λ was optimised to be $\lambda = 0.6$ on a train set with 10-fold validation. The full curve predictions are generated by fitting a quadratic spline through the capacity at the prediction cycle (current cycle number), predicted knee-onset, knee-point, and EOL. We emphasise that when the knees are predicted to take place before the prediction cycle one is currently at, a linear interpolation is used.

The plots also display prediction intervals which are constructed using 'forward-dropout' as described in [20]. The one cycle model can accurately predict the full curve from any cycle. We note that the error in the prediction reduces as the cell approaches its EOL. This last point is demonstrated clearly in Figure 2.

While the results presented in Figures 1 and 2 are for the e-forgetting one-cycle model with full cell history, we emphasise that the smoothing is an enhancement of the one-cycle model (that reduces variance and mitigates noise). The fact that cell history is not required enables the retrofitting of batteries in active deployment—for example, in EV fleets—where

the one-cycle model is able to provide meaningful predictions immediately. We argue that 'historyless' models are critical to the scaling and adoption of edge-cloud or other competing frameworks for (distributed) battery management.

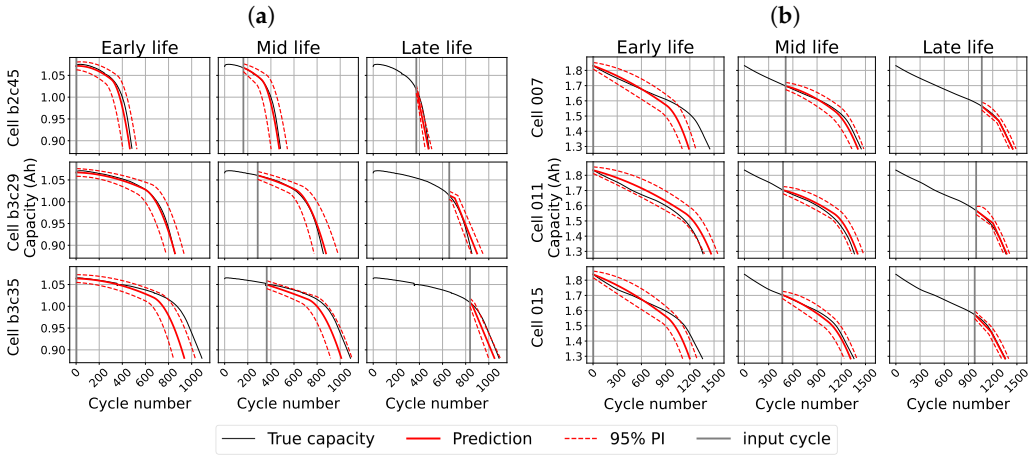

Figure 1. *e*-forgetting one-cycle model online prediction for three (randomly selected) test cells from each dataset. 'Early life' denotes prediction from cycle 3, 'Mid life'∼40% of life and 'Late life'∼80% of life. (**a**) Severson–Attia dataset; (**b**) Baumhöfer dataset.

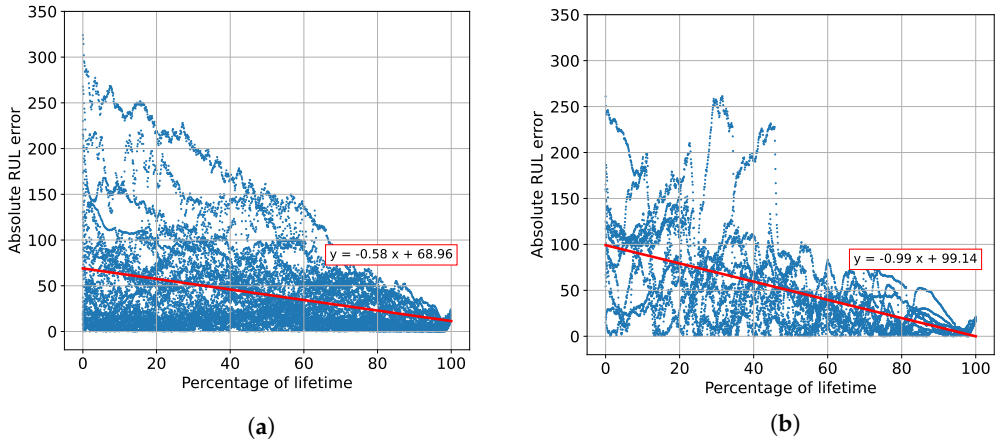

Figure 2. Error of RUL prediction compared with percentage of lifetime for test data (exponentially smoothed models). The red lines display a least squares linear regression fit through the points. (**a**) Severson–Attia dataset; (**b**) Baumhöfer dataset.

4.3. 2nd Life Assessment: Knee Region Classifier

The one-cycle model can predict RUL from any input cycle, in fact, the model predicts also the degradation trajectory from the input-cycle to RUL (cycle number). It does not require cycle number-specific information or data from multiple past cycles. For this reason, it has particular applicability to second-life applications.

Consider the following thought experiment: one wishes to purchase a used cell for a given application (e.g., stationary energy storage) but one does not know the specific history of the cell. Of particular interest is whether the cell has passed its knee and started rapid nonlinear capacity loss [13]. What one knows are the manufacturer's cell specifications and some qualitative knowledge that the cell was used in a way that fits the data used to train the model (recognisably, this is a heavy assumption, but a discussion on *model transfer* is left for future research). Given data for cells of the same type, a single high-throughput test cycle can be performed on the cell and the one-cycle model is used to predict the ttk-o, ttk-p and RUL. If the predicted ttk-p is negative, then this tells us that the cell has passed its knee-point.

The results of classifying test cells by proximity to knee-onset and point are displayed in Figure 3—the classes were chosen for demonstrative purposes and a more granular consideration is possible with the one-cycle model (for example the structure presented in [10] (Section 3) or [23]). We see that the model can accurately classify cells. The lowest accuracy is observed for classifying cells as between knee-onset and knee-point ('onset to knee'). This is explained by the narrowness of this band. A more granular consideration (such as that presented in Figure 2 for the RUL) would show that the model is still predicting within close proximity to the knee-onset and point when wrongly classifying cells as 'before onset'.

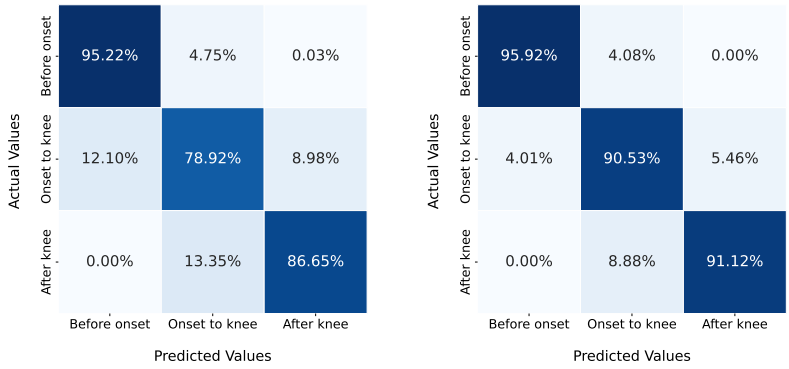

(**a**) (**b**)

Figure 3. Model's accuracy at classifying test cells by proximity to knee. Predictions were made from individual cycles. (**a**) Severson–Attia dataset; (**b**) Baumhöfer dataset.

4.4. Model Ensemble

A simple and natural approach to leveraging the full spectrum of signals and several available models is to create an ensemble model of models. Once the prediction of multiple models is available, one can then create an *ensemble model* by averaging predictions or by training a new model that takes as input the predictions of each model [71]. Ensemble learning is a commonly used approach to improve predictive performance, and in the literature, surrounding batteries has been used to improve the prediction of SOH [72,73].

Using the Severson–Attia dataset as input data, we tested an ensemble model combining the three models (see Section 3): exponentially smoothed (e-forgetting) one-cycle model of Section 4.2 (for the Severson–Attia dataset), cycle-to-cycle RVM model of [10], and the simple lookup model of Section 3.4 (using with $k = 3$ and the MAE metric (3)). As the lookup table-based model is a naive model with low in-sample performance it is given half weight compared to the other two models in the averaging, concretely,

$$\text{Ensemble} = \frac{2}{5} \times \text{'One-cycle } (e\text{-smoothing)'} + \frac{2}{5} \times \text{'RVM'} + \frac{1}{5} \times \text{'Lookup table'}.$$

Further optimisation of model weights is possible, for example, via cross-validation [74] or simply convex optimisation of weights (across the test set).

The performance metrics of each constituent model and the resulting ensemble model are presented in Table 4 where the predictions are made from cycle 200. We see that the ensemble model *outperforms any individual model* (see marked values), effectively reducing overfitting. Last, and left unexplored, is the recognition that the methodology of Section 3.2 could also be deployed for the ensemble model.

Table 4. Comparison of ensemble model with constituent models predicting from cycle 200. The Ensemble model outperforms each model individually as seen by the marked entries. Train metrics for the lookup table model are calculated using a leave-one-out approach. Metrics presented are for the Severson–Attia dataset.

	Knee-Onset				**Knee-Point**				**EOL**			
	RMSE (Cycles)		**MAPE (%)**		**RMSE (Cycles)**		**MAPE (%)**		**RMSE (Cycles)**		**MAPE (%)**	
Model	**Train**	**Test**	**Train**	**Test**	**Train**	**Test**	**Train**	**Test**	**Train**	**Test**	**Train**	**Test**
One-cycle (*e*-smoothing)	22	59	3.7	9.5	20	71	2.2	7.9	25	77	2.5	6.6
RVM	37	66	6.2	10.9	31	67	4.1	8.4	29	78	2.8	7.6
Lookup table	119	101	24.4	19.2	132	134	19.5	19.0	161	165	18.4	18.3
Ensemble	36	49	7.2	8.6	34	56	5.0	6.9	38	66	4.2	6.1

5. Conclusions and Outlook

In this work, the literature on one-cycle type models was reviewed. A particular benefit of the one-cycle model is that it does not require the history of the cell to make useful predictions and thus can additionally be used for cell selection. Recognising that the one-cycle model is deployed in the literature exclusively on the Attia–Severson dataset, we show that the methodology is of a wider scope by deploying it on the Baumhofer dataset. The cycling of cells in this dataset is different in nature to the cycling in Attia–Severson, including a much smaller amount of sample (48 vs. ∼160). To keep the message of this work focused, Internal Resistance prediction was only superficially discussed; nonetheless, the same analysis can be carried out—this has been exemplified upstream in [12,20].

By reflecting on the surging industry offering cloud platforms and solutions for battery data analysis, we imagined how one would leverage models like the one-cycle one within such frameworks. An exponential-smoothing model was proposed to include past information without storing complete data (voltage-current) with the critical benefit of reducing prediction variance and mitigating noise. The exponential-smoothing methodology of (1) is not tied to the one-cycle model as it can be overlaid over any model—it is thus a promising result of general interest.

Knowing that much of the existing individual literature contributions on lifetime prognostics present a single model development, we argue that the multiset cloud frameworks currently being developed in the market allow for many different models to be deployed (underpinned by the same dataset). Instead of choosing the best predictive model by approach and bespoke metric, a constructive solution is the ensemble of models. We consider ensemble learning as an approach to reduce overfitting and improve model performance and show that a simple weighted-average of models (including the field foundational lookup table method) can outperform the individual state-of-the-art model. The preliminary results presented are promising, and the authors view this area as a potentially fruitful avenue for future research. Other approaches could look at averaging more models with other approaches (i.e., that latch on to input signals in different ways) or consider training models jointly [71] (regression of models).

Another attractive feature of the ensemble approach is the ability to balance explainability with predictive power. 'Black box' approaches (such as NNs) are often criticised for lacking explainability albeit adding strong predictive power. Deployed in conjunction with an explainable model, the user can gain some understanding of the 'black box' model and the option to place more weight on the predictions made by an explainable model. Deployed in conjunction with an explainable model (in terms of how the model arrives at its decision and the contribution of predictors on targets), the ensemble model draws from the predictive power of the black box CNN and provides an overall model which is explainable (through weights assigned) when treating each component model as a variable.

6. Methods

Learning rate scheduler starting from the default Keras learning rate; the learning rate scheduler updates the learning every 'decay step' number of epochs as described in Equation (2)

$$\text{new learning rate} = \text{previous learning rate} \times \text{decay rate}. \tag{2}$$

Machine learning performance scores are the mean absolute error (MAE), mean absolute percentage error (MAPE), and root mean square error (RMSE) defined as follows, respectively: for $\boldsymbol{y}$ the vector of true knee/elbow-points (expressed in number of cycles) and $\hat{\boldsymbol{y}}$ is the vector of predicted values, then

$$\text{MAE}(\boldsymbol{y}, \hat{\boldsymbol{y}}) = \frac{1}{n_{\text{samples}}} \sum_{i=1}^{n_{\text{samples}}} |\hat{y}_i - y_i|, \tag{3}$$

$$\text{MAPE}(\boldsymbol{y}, \hat{\boldsymbol{y}}) = \frac{100\%}{n_{\text{samples}}} \sum_{i=1}^{n_{\text{samples}}} \frac{|\hat{y}_i - y_i|}{y_i}, \tag{4}$$

$$\text{RMSE}(\boldsymbol{y}, \hat{\boldsymbol{y}}) = \sqrt{\frac{1}{n_{\text{samples}}} \sum_{i=1}^{n_{\text{samples}}} (\hat{y}_i - y_i)^2}. \tag{5}$$

Author Contributions: All authors provided specific domain expertise. C.S., R.I. and G.d.R.: wrote, edited and reviewed the manuscript. G.d.R. supervised the work. All authors have read and agreed to the published version of the manuscript.

Funding: This project was funded by an industry-academia grant *EPSRC EP/R511687/1* awarded by *EPSRC & University of Edinburgh* program *Impact Acceleration Account (IAA)*. R. Ibraheem is a Ph.D. student in EPSRC's MAC-MIGS Centre for Doctoral Training. MAC-MIGS is supported by the UK's Engineering and Physical Science Research Council (grant number EP/S023291/1). G. dos Reis acknowledges partial support from the *Fundação para a Ciência e a Tecnologia* (Portuguese Foundation for Science and Technology) through the project UIDB/00297/2020 and UIDP/00297/2020 (Center for Mathematics and Applications, CMA/FCT/UNL). G. dos Reis acknowledges support from the Faraday Institution [grant number FIRG049].

Data Availability Statement: All data used in this work is already publicly available. No new data was generated.

Acknowledgments: The authors would like to thank Hang Ruan and Richard Gilchrist for the helpful discussions.

Conflicts of Interest: The authors declare no conflict of interest.

References

1. Li, A.G.; West, A.C.; Preindl, M. Towards unified machine learning characterization of lithium-ion battery degradation across multiple levels: A critical review. *Appl. Energy* **2022**, *316*, 119030. [CrossRef]
2. Tian, J.; Xiong, R.; Shen, W. A review on state of health estimation for lithium ion batteries in photovoltaic systems. *eTransportation* **2019**, *2*, 100028. [CrossRef]
3. Nuroldayeva, G.; Serik, Y.; Adair, D.; Uzakbaiuly, B.; Bakenov, Z. State of Health Estimation Methods for Lithium-Ion Batteries. *Int. J. Energy Res.* **2023**, *2023*, 21. [CrossRef]
4. Joshi, U.D.; Gambhir, A.V.; Mandhana, A. *Machine Learning Approaches for Lithium-Ion Battery Health Parameters Estimation*; Technical Report; SAE Technical Paper; SAE International: Warrendale, PA, USA, 2022.
5. Wang, S.; Jin, S.; Deng, D.; Fernandez, C. A critical review of online battery remaining useful lifetime prediction methods. *Front. Mech. Eng.* **2021**, *7*, 719718. [CrossRef]
6. Su, L.; Wu, M.; Li, Z.; Zhang, J. Cycle life prediction of lithium-ion batteries based on data-driven methods. *eTransportation* **2021**, *10*, 100137. [CrossRef]
7. Guo, W.; Sun, Z.; Vilsen, S.B.; Meng, J.; Stroe, D.I. Review of "grey box" lifetime modeling for lithium-ion battery: Combining physics and data-driven methods. *J. Energy Storage* **2022**, *56*, 105992. [CrossRef]

8. Finegan, D.P.; Zhu, J.; Feng, X.; Keyser, M.; Ulmefors, M.; Li, W.; Bazant, M.Z.; Cooper, S.J. The application of data-driven methods and physics-based learning for improving battery safety. *Joule* **2021**, *5*, 316–329. [CrossRef]
9. Celik, B.; Sandt, R.; dos Santos, L.C.P.; Spatschek, R. Prediction of Battery Cycle Life Using Early-Cycle Data, Machine Learning and Data Management. *Batteries* **2022**, *8*, 266. [CrossRef]
10. Fermín, P.; McTurk, E.; Allerhand, M.; Medina-Lopez, E.; Anjos, M.F.; Sylvester, J.; dos Reis, G. Identification and machine learning prediction of knee-point and knee-onset in capacity degradation curves of lithium-ion cells. *Energy AI* **2020**, *1* , 100006. [CrossRef]
11. Sohn, S.; Byun, H.E.; Lee, J.H. Two-stage deep learning for online prediction of knee-point in Li-ion battery capacity degradation. *Appl. Energy* **2022**, *328*, 120204. [CrossRef]
12. Strange, C.; Li, S.; Gilchrist, R.; dos Reis, G. Elbows of Internal Resistance Rise Curves in Li-Ion Cells. *Energies* **2021**, *14*, 1206. [CrossRef]
13. Attia, P.M.; Bills, A.A.; Brosa Planella, F.; Dechent, P.; dos Reis, G.; Dubarry, M.; Gasper, P.; Gilchrist, R.; Greenbank, S.; Howey, D.; et al. Review—"Knees" in Lithium-Ion Battery Aging Trajectories. *J. Electrochem. Soc.* **2022**, *169* , 060517. [CrossRef]
14. Paulson, N.H.; Kubal, J.; Ward, L.; Saxena, S.; Lu, W.; Babinec, S.J. Feature engineering for machine learning enabled early prediction of battery lifetime. *J. Power Sources* **2022**, *527*, 231127. [CrossRef]
15. Severson, K.; Attia, P.; Jin, N.; Perkins, N.; Jiang, B.; Yang, Z.; Chen, M.; Aykol, M.; Herring, P.; Fraggedakis, D.; et al. Data-driven prediction of battery cycle life before capacity degradation. *Nat. Energy* **2019**, *4*, 383–391. [CrossRef]
16. Greenbank, S.; Howey, D. Automated Feature Extraction and Selection for Data-Driven Models of Rapid Battery Capacity Fade and End of Life. *IEEE Trans. Ind. Inform.* **2022**, *18*, 2965–2973. [CrossRef]
17. Saxena, S.; Ward, L.; Kubal, J.; Lu, W.; Babinec, S.; Paulson, N. A convolutional neural network model for battery capacity fade curve prediction using early life data. *J. Power Sources* **2022**, *542*, 231736. [CrossRef]
18. Rieger, L.H.; Flores, E.; Nielsen, K.F.; Norby, P.; Ayerbe, E.; Winther, O.; Vegge, T.; Bhowmik, A. Uncertainty-aware and explainable machine learning for early prediction of battery degradation trajectory. *Digit. Discov.* **2023**, *2*, 112–122. [CrossRef]
19. Li, W.; Sengupta, N.; Dechent, P.; Howey, D.; Annaswamy, A.; Sauer, D.U. One-shot battery degradation trajectory prediction with deep learning. *J. Power Sources* **2021**, *506*, 230024. [CrossRef]
20. Strange, C.; dos Reis, G. Prediction of future capacity and internal resistance of Li-ion cells from one cycle of input data. *Energy AI* **2021**, *5*, 100097. [CrossRef]
21. Li, W.; Zhang, H.; van Vlijmen, B.; Dechent, P.; Sauer, D.U. Forecasting battery capacity and power degradation with multi-task learning. *Energy Storage Mater.* **2022**, *53*, 453–466. [CrossRef]
22. Ibraheem, R.; Strange, C.; dos Reis, G. Capacity and Internal Resistance of lithium-ion batteries: Full degradation curve prediction from Voltage response at constant Current at discharge. *J. Power Sources* **2023**, *556*, 232477. [CrossRef]
23. Sohn, S.; Byun, H.E.; Lee, J.H. CNN-based Online Diagnosis of Knee-point in Li-ion Battery Capacity Fade Curve. In Proceedings of the 13th IFAC Symposium on Dynamics and Control of Process Systems, including Biosystems DYCOPS, Busan, Republic of Korea, 14–17 June 2022; IFAC-PapersOnLine: Amsterdam, The Netherlands, 2022; Volume 55, pp. 181–185. [CrossRef]
24. Kim, K.; Kim, M.; Churr, H.; Lee, G.; Han, S. G-K curve-based knee point prediction method for Li-ion batteries. In Proceedings of the 2021 21st International Conference on Control, Automation and Systems (ICCAS), Jeju, Republic of Korea, 12–15 October 2021; pp. 1190–1193. [CrossRef]
25. LeDell, E.; Poirier, S. H_2O automl: Scalable automatic machine learning. In Proceedings of the AutoML Workshop at ICML, Virtual Event, 13–18 July 2020; Volume 2020.
26. Zhang, C.; Zhao, S.; He, Y. An integrated method of the future capacity and RUL prediction for lithium-ion battery pack. *IEEE Trans. Veh. Technol.* **2021**, *71*, 2601–2613. [CrossRef]
27. Zhao, S.; Zhang, C.; Wang, Y. Lithium-ion battery capacity and remaining useful life prediction using board learning system and long short-term memory neural network. *J. Energy Storage* **2022**, *52*, 104901. [CrossRef]
28. Zhang, H.; Su, Y.; Altaf, F.; Wik, T.; Gros, S. Interpretable Battery Cycle Life Range Prediction Using Early Cell Degradation Data. *IEEE Trans. Transp. Electrif.* **2022**, *1*. [CrossRef]
29. Amey, J.L.; Keeley, J.; Choudhury, T.; Kuprov, I. Neural network interpretation using descrambler groups. *Proc. Natl. Acad. Sci. USA* **2021**, *118*, e2016917118. [CrossRef]
30. Ma, Y.; Wu, L.; Guan, Y.; Peng, Z. The capacity estimation and cycle life prediction of lithium-ion batteries using a new broad extreme learning machine approach. *J. Power Sources* **2020**, *476*, 228581. [CrossRef]
31. Shen, S.; Nemani, V.; Liu, J.; Hu, C.; Wang, Z. A Hybrid Machine Learning Model for Battery Cycle Life Prediction with Early Cycle Data. In Proceedings of the 2020 IEEE Transportation Electrification Conference & Expo (ITEC), IEEE, Chicago, IL, USA, 21–25 June 2021; pp. 181–184.
32. Yang, F.; Wang, D.; Xu, F.; Huang, Z.; Tsui, K.L. Lifespan prediction of lithium-ion batteries based on various extracted features and gradient boosting regression tree model. *J. Power Sources* **2020**, *476*, 228654. [CrossRef]
33. Diao, W.; Saxena, S.; Han, B.; Pecht, M. Algorithm to Determine the Knee Point on Capacity Fade Curves of Lithium-Ion Cells. *Energies* **2019**, *12*, 2910. [CrossRef]
34. Jones, P.K.; Stimming, U.; Lee, A.A. Impedance-based forecasting of lithium-ion battery performance amid uneven usage. *Nat. Commun.* **2022**, *13*, 4806. [CrossRef]

35. Tian, J.; Xiong, R.; Shen, W.; Lu, J. Data-driven battery degradation prediction: Forecasting voltage-capacity curves using one-cycle data. *EcoMat* **2022**, *4* , e12213. [CrossRef]
36. Planella, F.B.; Sheikh, M.; Widanage, W.D. Systematic derivation and validation of a reduced thermal-electrochemical model for lithium-ion batteries using asymptotic methods. *Electrochim. Acta* **2021**, *388*, 138524. [CrossRef]
37. Chen, C.H.; Planella, F.B.; O'regan, K.; Gastol, D.; Widanage, W.D.; Kendrick, E. Development of experimental techniques for parameterization of multi-scale lithium-ion battery models. *J. Electrochem. Soc.* **2020**, *167*, 080534. [CrossRef]
38. Ecker, M.; Tran, T.K.D.; Dechent, P.; Käbitz, S.; Warnecke, A.; Sauer, D.U. Parameterization of a physico-chemical model of a lithium-ion battery: I. Determination of parameters. *J. Electrochem. Soc.* **2015**, *162*, A1836. [CrossRef]
39. Ecker, M.; Käbitz, S.; Laresgoiti, I.; Sauer, D.U. Parameterization of a physico-chemical model of a lithium-ion battery: II. Model validation. *J. Electrochem. Soc.* **2015**, *162*, A1849. [CrossRef]
40. Park, S.; Kato, D.; Gima, Z.; Klein, R.; Moura, S. Optimal experimental design for parameterization of an electrochemical lithium-ion battery model. *J. Electrochem. Soc.* **2018**, *165*, A1309. [CrossRef]
41. Liu, H.; Bie, C.; Luo, F.; Kang, J.; Zhang, Y. Rapid Prediction of Retired Ni-MH Batteries Capacity Based on Reliable Multi-Parameter Driven Analysis. *Energies* **2022**, *15*, 9156. [CrossRef]
42. Ruan, H.; Xiao, P.; Xiao, L.; Kelly, J.R. Joint Iterative Optimization-Based Low-Complexity Adaptive Hybrid Beamforming for Massive MU-MIMO Systems. *IEEE Trans. Commun.* **2021**, *69*, 1707–1722. [CrossRef]
43. Hu, J.; Morais, H.; Sousa, T.; Lind, M. Electric vehicle fleet management in smart grids: A review of services, optimization and control aspects. *Renew. Sustain. Energy Rev.* **2016**, *56*, 1207–1226. [CrossRef]
44. You, S.; Hu, J.; Ziras, C. An overview of modeling approaches applied to aggregation-based fleet management and integration of plug-in electric vehicles. *Energies* **2016**, *9*, 968. [CrossRef]
45. von Bülow, F.; Heinrich, F.; Meisen, T. Fleet Management Approach for Manufacturers displayed at the Use Case of Battery Electric Vehicles. In Proceedings of the 2021 IEEE International Conference on Systems, Man, and Cybernetics (SMC), Melbourne, Australia, 17–20 October 2021; pp. 3218–3225.
46. Kumtepeli, V.; Howey, D.A. Understanding battery aging in grid energy storage systems. *Joule* **2022**, *6*, 2250–2252. [CrossRef]
47. Reniers, J.M.; Howey, D.A. Digital twin of a MWh-scale grid battery system for efficiency and degradation analysis. *Appl. Energy* **2023**, *336*, 120774. [CrossRef]
48. Mohamed, A.; Ruan, H.; Abdelwahab, M.H.H.; Dorneanu, B.; Xiao, P.; Arellano-Garcia, H.; Gao, Y.; Tafazolli, R. An Inter-Disciplinary Modelling Approach in Industrial 5G/6G and Machine Learning Era. In Proceedings of the 2020 IEEE International Conference on Communications Workshops (ICC Workshops), Dublin, Ireland, 7–11 June 2020; pp. 1–6.
49. Gubbi, J.; Buyya, R.; Marusic, S.; Palaniswami, M. Internet of Things (IoT): A vision, architectural elements, and future directions. *Future Gener. Comput. Syst.* **2013**, *29*, 1645–1660. [CrossRef]
50. Samanta, A.; Williamson, S.S. A Survey of Wireless Battery Management System: Topology, Emerging Trends, and Challenges. *Electronics* **2021**, *10*, 2193. [CrossRef]
51. Sulzer, V.; Mohtat, P.; Aitio, A.; Lee, S.; Yeh, Y.T.; Steinbacher, F.; Khan, M.U.; Lee, J.W.; Siegel, J.B.; Stefanopoulou, A.G.; et al. The challenge and opportunity of battery lifetime prediction from field data. *Joule* **2021**, *5*, 1934–1955. [CrossRef]
52. Song, L.; Zhang, K.; Liang, T.; Han, X.; Zhang, Y. Intelligent state of health estimation for lithium-ion battery pack based on big data analysis. *J. Energy Storage* **2020**, *32*, 101836. [CrossRef]
53. Li, W.; Sengupta, N.; Dechent, P.; Howey, D.; Annaswamy, A.; Sauer, D.U. Online capacity estimation of lithium-ion batteries with deep long short-term memory networks. *J. Power Sources* **2021**, *482*, 228863. [CrossRef]
54. Yao, L.; Xu, S.; Tang, A.; Zhou, F.; Hou, J.; Xiao, Y.; Fu, Z. A Review of Lithium-Ion Battery State of Health Estimation and Prediction Methods. *World Electr. Veh. J.* **2021**, *12*, 113. [CrossRef]
55. Huang, Y.; Lu, Y.; Wang, F.; Fan, X.; Liu, J.; Leung, V.C. An Edge Computing Framework for Real-Time Monitoring in Smart Grid. In Proceedings of the 2018 IEEE International Conference on Industrial Internet (ICII), Bellevue, WA, USA, 21–23 October 2018; pp. 99–108. [CrossRef]
56. Albataineh, H.; Nijim, M.; Bollampall, D. The Design of a Novel Smart Home Control System using Smart Grid Based on Edge and Cloud Computing. In Proceedings of the 2020 IEEE 8th International Conference on Smart Energy Grid Engineering (SEGE), Oshawa, ON, Canada, 12–14 August 2020; pp. 88–91. [CrossRef]
57. Feng, C.; Wang, Y.; Chen, Q.; Ding, Y.; Strbac, G.; Kang, C. Smart grid encounters edge computing: Opportunities and applications. *Adv. Appl. Energy* **2021**, *1*, 100006. [CrossRef]
58. Sarroca, P.G.; Sánchez-Artigas, M. MLLess: Achieving Cost Efficiency in Serverless Machine Learning Training. *arXiv* **2022**, arXiv:2206.05786.
59. Hui, H.; Ding, Y.; Shi, Q.; Li, F.; Song, Y.; Yan, J. 5G network-based Internet of Things for demand response in smart grid: A survey on application potential. *Appl. Energy* **2020**, *257*, 113972. [CrossRef]
60. Borgaonkar, R.; Anne Tøndel, I.; Zenebe Degefa, M.; Gilje Jaatun, M. Improving smart grid security through 5G enabled IoT and edge computing. *Concurr. Comput. Pract. Exp.* **2021**, *33*, e6466. [CrossRef]
61. Lei, L.; Chen, Q.; Pei, S.; Maharjan, S.; Yan, Z. Vehicular Edge Computing and Networking: A Survey. *Mob. Netw. Appl.* **2021**, *26*, 1145–1168. [CrossRef]
62. Gu, X.; Zhang, G. Energy-efficient computation offloading for vehicular edge computing networks. *Comput. Commun.* **2021**, *166*, 244–253. [CrossRef]

63. Jiang, Z.; Li, H.; Qu, Z.; Zhang, J. Recent progress in lithium-ion battery thermal management for a wide range of temperature and abuse conditions. *Int. J. Hydrogen Energy* **2022**, *47*, 9428–9459. [CrossRef]
64. Baumhöfer, T.; Brühl, M.; Rothgang, S.; Sauer, D.U. Production caused variation in capacity aging trend and correlation to initial cell performance. *J. Power Sources* **2014**, *247*, 332–338. [CrossRef]
65. Sauer, D.U. Time-Series Cyclic Aging Data on 48 Commercial NMC/Graphite Sanyo/Panasonic UR18650E Cylindrical Cells. 2021. Available online: https://publications.rwth-aachen.de/record/818642 (accessed on 15 February 2023).
66. dos Reis, G.; Strange, C.; Yadav, M.; Li, S. Lithium-ion battery data and where to find it. *Energy AI* **2021**, *5*, 100081. [CrossRef]
67. Strange, C.; Allerhand, M.; Dechent, P.; dos Reis, G. Automatic method for the estimation of Li-ion degradation test sample sizes required to understand cell-to-cell variability. *Energy AI* **2022**, *9*, 100174. [CrossRef]
68. Attia, P.M.; Grover, A.; Jin, N.; Severson, K.A.; Markov, T.M.; Liao, Y.H.; Chen, M.H.; Cheong, B.; Perkins, N.; Yang, Z.; et al. Closed-loop optimization of fast-charging protocols for batteries with machine learning. *Nature* **2020**, *578*, 397–402. [CrossRef]
69. Dechent, P.; Greenbank, S.; Hildenbrand, F.; Jbabdi, S.; Sauer, D.U.; Howey, D.A. Estimation of Li-Ion Degradation Test Sample Sizes Required to Understand Cell-to-Cell Variability. *Batter. Supercaps* **2021**, *4*, 1821–1829. [CrossRef]
70. Gasper, P.; Collath, N.; Hesse, H.C.; Jossen, A.; Smith, K. Machine-Learning Assisted Identification of Accurate Battery Lifetime Models with Uncertainty. *J. Electrochem. Soc.* **2022**, *169*, 080518. [CrossRef]
71. Sagi, O.; Rokach, L. Ensemble learning: A survey. *Wiley Interdiscip. Rev. Data Min. Knowl. Discov.* **2018**, *8*, e1249. [CrossRef]
72. Shen, S.; Sadoughi, M.; Li, M.; Wang, Z.; Hu, C. Deep convolutional neural networks with ensemble learning and transfer learning for capacity estimation of lithium-ion batteries. *Appl. Energy* **2020**, *260*, 114296. [CrossRef]
73. Gou, B.; Xu, Y.; Feng, X. An Ensemble Learning-based Data-Driven Method for Online State-of-Health Estimation of Lithium-ion Batteries. *IEEE Trans. Transp. Electrif.* **2020**, *7*, 422–436. [CrossRef]
74. Berrar, D. Cross-Validation. In *Encyclopedia of Bioinformatics and Computational Biology*; Ranganathan, S., Gribskov, M., Nakai, K., Schönbach, C., Eds.; Academic Press: Oxford, UK, 2019; pp. 542–545. [CrossRef]